UTRECHT UNIVERSITY

INSTITUTE FOR MARINE AND ATMOSPHERIC RESEARCH UTRECHT

MASTER'S THESIS

Differences between Arctic interannual and decadal variability across climate states

Author:
Jesse REUSEN

Supervisors:
Eveline VAN DER LINDEN[1]
Richard BINTANJA[1,3]
Michiel VAN DEN BROEKE[2]

July 6, 2018

[1]Royal Netherlands Meteorological Institute
[2]Utrecht University
[3]University of Groningen

Abstract

Understanding natural climate fluctuations is of vital importance in a globally warming world. These climate variations may amplify or dampen (human-induced) trends in temperature, even more so since variability itself may change with a changing climate. Here, we quantify the magnitude and other characteristics of interannual to decadal variability in Arctic temperature and their dependence on the climate state. Moreover, we identify the processes responsible for the state-dependency of the variations, using a state-of-the-art global climate model with which five quasi-equilibrium climate states with one-fourth, halved, present-day, doubled and quadrupled atmospheric CO_2 forcing have been simulated. The main reasons behind the natural fluctuations in Arctic temperature including their dependence on the state of the climate are linked to anomalous atmospheric and oceanic heat transport towards the Arctic. Correlations of Arctic surface air temperature with poleward atmospheric and oceanic transports are strongly dependent on the time scale of the variations. Model results suggest that atmospheric heat transport leads (and also controls) Arctic temperature variations on interannual timescales, whereas oceanic transport is found to govern the fluctuations on decadal timescales. This time-scale transition of atmospheric to oceanic dominance for Arctic temperature variations is most obvious when there is interannual to decadal variability in Arctic sea ice cover. In warm climates (without Arctic sea ice cover), there is no correlation between oceanic transport and temperature on any timescale. In cold climates (with full Arctic sea ice cover), interaction between ocean and atmosphere is limited, suggesting that poleward atmosperic heat transport is the primary driver on all timescales (interannual and decadal).

1 Introduction

In the last few decades, the climate is warming globally at a rate of ~ 0.17 °C per decade (Hansen et al., 2010). This rate of warming can be obscured by naturally occurring climate fluctuations, which are superimposed on the trend. Natural fluctuations are present on all timescales, ranging from daily (day / night) variations to interannual and decadal variations. In this paper, we address interannual and decadal climate variability of the Arctic region, where trends and variability are generally largest.

Throughout history, the earth has experienced various successive stages of warm and cold climates. For instance, during the Last Glacial Maximum (about 21 kyr B.P.), global temperatures were 3-5°C lower as compared to the pre-industrial climate (Field et al., 2014), and about 10 °C lower in the Northern Hemispheric midlatitudes (Bintanja et al., 2005). Model simulations of the Last Glacial Maximum show that the expansion of ice sheets over North America and Eurasia caused strong changes in oceanic and atmospheric circulations (Ganopolski et al., 1998). The most recent period, known as the Holocene, experienced several millennial, centennial and decadal scale cooling events, which also involved large scale ocean and atmosphere reorganizations (Ortiz et al., 2000; Mayewski et al., 2004). Clearly, atmospheric and oceanic processes and the resulting natural climate variability are strongly dependent on the state of the climate.

The Arctic climate is very sensitive to climate forcing through the action of specific climate feedbacks (mainly the ice-albedo and lapse-rate feedbacks). Models and observations show that for greenhouse forcing the Arctic warms 2 to 3 times as fast compared to the rest of the world (Holland and Bitz, 2003; Comiso and Hall, 2014), but also that the temporal variability is higher (Chylek et al., 2011). To accurately estimate the long-term (human-induced) climate trends, understanding and quantifying the variations superimposed on this trend is a necessity. When the climate changes, for instance due to an increase or decrease of the CO_2 concentration in the atmosphere, these natural climate fluctuations may change as well. Since fluctuations can obscure or amplify long-term trends, understanding the frequency, amplitude and relevant climate mechanisms, and the changes therein, is vital.

Processes driving variability in the Arctic region each act on their own typical timescale. Consequently, processes controlling interannual variability may well differ from those associated with decadal variability. Therefore, it is important to study dominant processes active on both timescales. These governing mechanisms can effectively be subdivided in either atmospheric or oceanic processes. In this paper, the influence of anomalous heat transport through either the ocean or the atmosphere on Arctic climate variability is investigated. For decadal to multidecadal variations, it has been shown that ocean heat transport anomalies modulate sea ice cover and surface heat fluxes, with the atmosphere responding by modifying pressure patterns and circulation dynamics (e.g. Jungclaus and Koenigk, 2010; Kinnard et al., 2011; Årthun and Eldevik, 2016). Variability in the atmosphere is often represented by using various modes, such as the North Atlantic Oscillation (NAO) (Hurrell et al., 2003; Holland, 2003) and the Pacific Decadal Oscillation (PDO) (Mantua and Hare, 2002; Day et al., 2012). On interannual time scales, a link was found between wintertime NAO and Arctic sea ice cover, both in models (Caian et al., 2018) and observations (Frankignoul et al., 2014). Additionally, findings by Zhang and Li (2017) suggest that the interannual variability in Arctic sea ice concentration is related to anomalies in the large-scale tropospheric circulation over the Northern Hemisphere, although they did not consider the importance of oceanic processes on the interannual variability in sea ice concentration. Nevertheless, these findings suggest that variations on interannual timescales are most likely associated with processes in the atmosphere, whereas anomalies in ocean heat transport have a comparatively strong impact on decadal and multi-decadal timescales.

Sea ice also plays a key role in Arctic climate variability (Rind et al., 1997; Screen and Simmonds, 2010), by inhibiting exchange of heat and moisture between the ocean and the atmosphere (Selivanova et al., 2016), as well as by its contribution to the ice-albedo feedback. To date, most research in Arctic climate variability has focused on Arctic decadal variability (e.g. Day et al., 2012; van der Linden et al., 2017), with less attention to interannual variations. In this paper, timescales ranging from interannual to multi-decadal are considered, with a primary focus on quantifying and understanding the differences between these in terms of the governing processes.

2 Methods

2.1 The model

In this paper the dependence of Arctic interannual to decadal variability on the state of the climate is investigated. For that we need long climate records, which unfortunately are not available from observations. We therefore use a state-of-the-art global climate model (EC-Earth) (Hazeleger et al., 2012). Five long (550-years) simulations have been carried out for the current climate as well as for two colder and two warmer climates. Version 2.3 of EC-Earth is used, which also contributed to the Coupled Model Intercomparison Project phase 5 (CMIP5) (Taylor et al., 2012). EC-Earth is a fully coupled global climate system model, consisting of atmospheric, oceanic and land surface modules. The atmospheric model is the Integrated Forecast System (IFS) of the European Center for Medium-range Weather forecasts, operating at a spectral resolution of T159 with 62 vertical levels, which contains the land module H-TESSEL (Balsamo et al., 2009). The oceanic model is the Nucleus for European Modelling of the Ocean (NEMO) model (Madec, 2008), developed by the Institute Pierre Simon Laplace (IPSL). It has a horizontal resolution of about 1 degrees and contains 42 vertical levels. Incorporated in NEMO is the Louvain la Neuve sea ice model version 2 (LIM2) (Fichefet and Maqueda, 1997; Goosse and Fichefet, 1999), which is a dynamic-thermodynamic sea ice model. Coupling of the atmospheric and oceanic components is performed using the OASIS (Ocean, Atmosphere, Sea Ice, Soil) coupling module (Valcke et al., 2003).

The simulation uses a spin-up of roughly a thousand years of pre-industrial forcing, followed by 44 years of spin-up with present-day forcing. Hereafter, the CO_2 concentration is instantaneously set to a fixed value. In the five simulations used here, the carbon dioxide (CO_2) concentration in the atmosphere is set to 0.25x, 0.5x, 1x, 2x and 4x the value of the year 2000 (present-day). Each simulation is then run for 550 years. During the last 450 years of each simulation, the climate is assumed to be in a quasi-equilibrium state (Figure 1); the first 100 years are considered spin-up to the respective climate states and are not be used in the analysis.

To remove any remaining trend in the five 450-year time series, all data is linearly detrended prior to the analyses. Changes in Arctic climate variability can then be studied in warmer or colder climates by comparing results to the control run. In this way, the changes in amplitude and frequency of the Arctic climate fluctuations and the processes responsible for this can be quantified and linked to the relevant climate mechanisms.

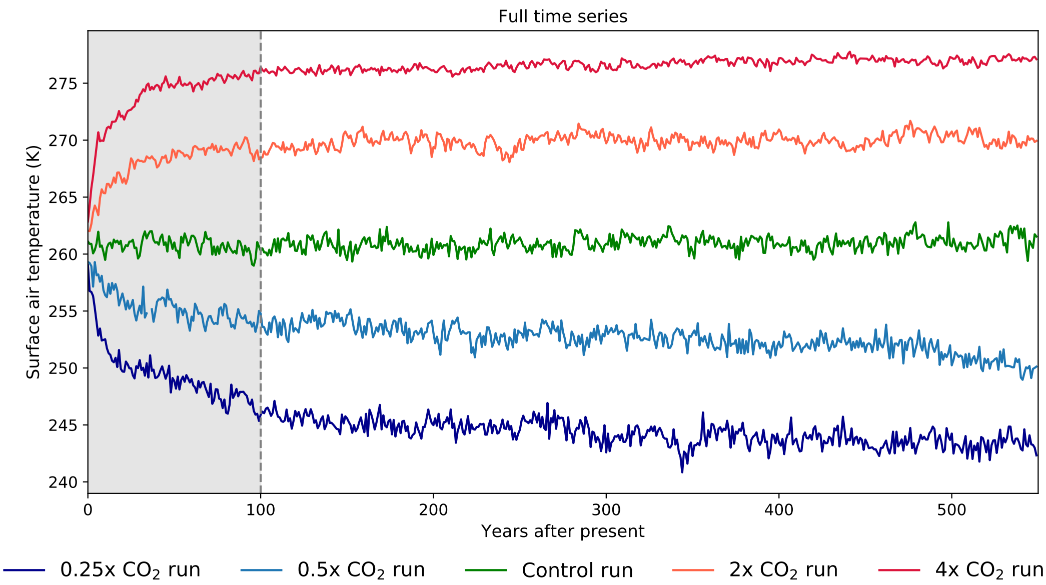

Figure 1 – Full time series of the Arctic surface air temperature for each simulation. The non-shaded area is used in the rest of the analyses, since the temperature is assumed to be in quasi-equilibrium after 100 years.

In this paper, high and low frequency variations (interannual vs. decadal) are analysed separately. This is achieved by applying a fourth-order Butterworth filter. Low (high) frequencies are filtered using a fourth order high-pass (low-pass) filter with a cut-off frequency of 0.1 yr^{-1}. Its effect is illustrated in Figure 2, which shows Arctic sea ice area anomalies of the detrended time series of the 0.25x CO_2 run. Figure 2a exhibits the effect of filtering decadal variations, whereas in Figure 2b the interannual variations have been removed. In this study, we henceforth consider all fluctuations with time scales under 10 years interannual, and anything longer than 10 years decadal. We acknowledge that this choice is somewhat arbitrary, but small changes in this choice should not affect the outcomes and conclusions of this study.

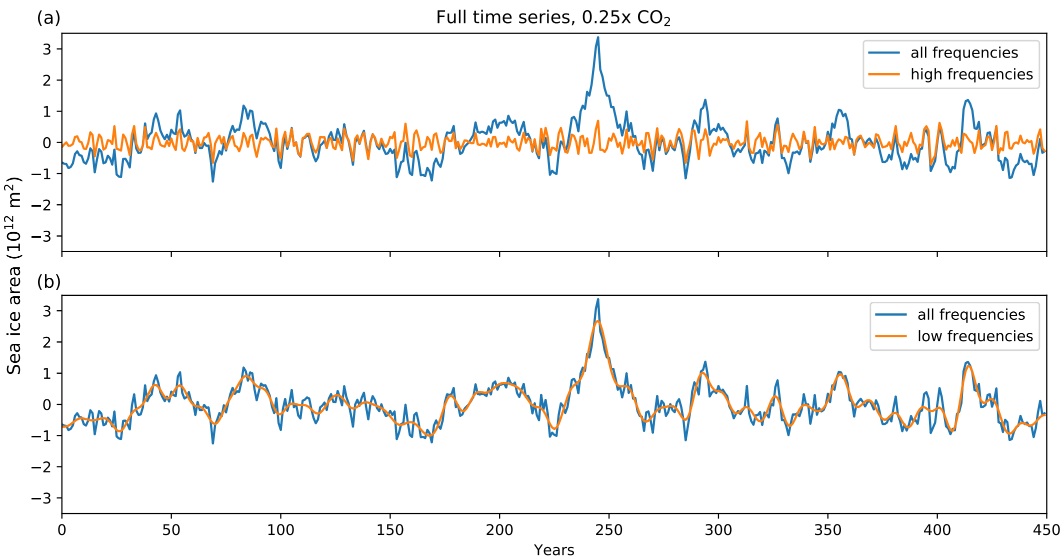

Figure 2 – Effect of the high-pass (a) and low-pass (b) Butterworth frequency filter with a cut-off frequency of 0.1 yr^{-1} on the full time series of the sea ice area in the 0.25x CO_2 run.

2.2 Arctic heat budget

This section sketches the theoretical background of the energy budget. The energy budget of the Arctic as given in Nakamura and Oort (1988) and Serreze et al. (2007) is:

$$\frac{\partial E_{\text{atm}}}{\partial t} = F_{\text{TOA}} - F_{\text{SFC}} - \nabla \cdot AHT \tag{1}$$

For the atmosphere, the net heat gain or loss $\left(\frac{\partial E_{\text{atm}}}{\partial t}\right)$ is the sum of the net flux at the top of the atmosphere (F_{TOA}), the net flux at the surface (F_{SFC}) and the convergence of the atmospheric heat transport at the sides ($-\nabla \cdot AHT$), as shown in Figure 3. The assumption that the climates are in semi-steady state holds true for the atmosphere, meaning that there is no net storage of heat in the atmosphere in the Arctic on time scales of one year or longer. In other words, $\frac{\partial E_{\text{atm}}}{\partial t} = 0$. The net flux at the top of the atmosphere and the net surface flux can be evaluated easily from the individual fluxes, as calculated by the EC-Earth model. The atmospheric heat transport can then be calculated as the net of F_{TOA} and F_{SFC}. The fluxes at the top of the atmosphere and at the surface are defined as positive downwards and the atmospheric heat transport is defined positive when directed northward, consistent with the schematic drawing in Figure 3.

Similarly, the energy budget of the ocean can be expressed as:

$$\frac{\partial E_{\text{oc}}}{\partial t} = F_{\text{SFC}} - \nabla \cdot OHT \tag{2}$$

The energy heat gain or loss of the ocean is the sum of the net flux at the surface and the convergence of the ocean heat transport through the sides ($-\nabla \cdot OHT$). For the ocean, because of its larger inertia, the steady-state assumption does not hold. Therefore, storage of energy over time scales of one year or more, $\frac{\partial E_{\text{oc}}}{\partial t}$, cannot be neglected. This term is henceforth evaluated as the change in ocean heat content in the Arctic over time (Dijkstra, 2008):

$$E_{\text{oc}} = \rho_0 c_p \int T dz \tag{3}$$

Where $\rho_0 = 1035$ kg/m^3 is the reference density of seawater, $c_p = 3992$ J Kg^{-1}K^{-1} is the heat capacity of seawater and T is the temperature at a certain depth. The total Arctic Ocean heat content is obtained by multiplying with the total ocean area North of 70 °N, since in our definition the Arctic spans the region from 70 to 90°N. The convergence of the ocean heat transport is subsequently calculated as the residual of the net surface fluxes and the time derivative of the ocean heat content.

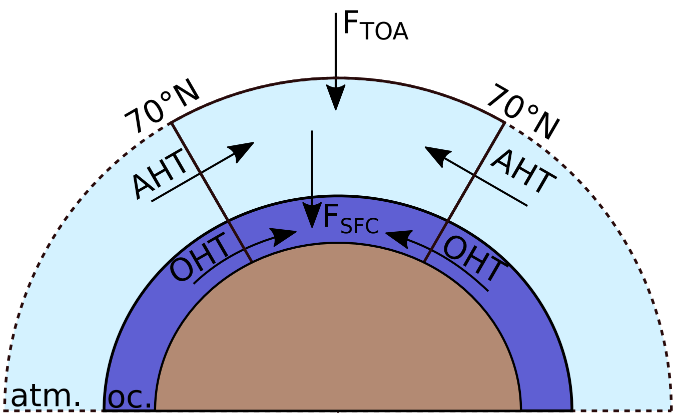

Figure 3 – Schematic view of the energy budget in the Arctic

3 Results

3.1 Global characteristics and validation

3.1.1 Mean State

Simulation	0.25x CO_2	0.5x CO_2	control	2x CO_2	4x CO_2	Obs. based
T_{DJF}	226.9	237.5	248.8	263.6	272.0	249.8
T_{JJA}	266.7	270.7	273.8	277.2	282.4	274.2
SIA_{max}	27.8	21.1	15.8	10.9	0.61	11.5
SIA_{min}	17.7	12.0	5.37	0.14	0.12	4.76

Table 1 – Simulation name, mean Arctic temperature in K in summer (T_{JJA}) and winter (T_{DJF}) and the sea ice area in 10^{12} m^2 in September (SIA_{min}) and March (SIA_{max}), respectively. Estimates of observationally-driven reanalyses products[1] have been added for comparison.

Due to the lack of long observational records of the Arctic climate, we use the EC-Earth model to evaluate climate variability. The inherent assumption is that EC-Earth accurately represents the real climate system. In this section we use observationally-driven reanalyses data to infer how good this assumption is for the Arctic climate and its variability.

The atmospheric CO_2 concentration exhibits a non linear relationship with both temperature and sea ice area, because radiative forcing depends roughly on the logarithm of atmospheric CO_2-content. This is clearly illustrated in Table 1, which shows Arctic mean temperature for summer and winter, as well as the average maximum and minimum sea ice area. Data averaged over observation based models has been added for comparison. Overall, the surface air temperature in the control run of EC-Earth is 0.4 degrees lower in winter and about 1 degrees lower in summer as compared to results obtained from the observation based models. The maximum and minimum sea ice area are larger in EC-Earth, as anticipated considering the lower average temperatures. In fact, the average sea ice area is heavily overestimated by the EC-Earth model. Differences are larger in winter (4.5 million square kilometers) than in summer (about 1 million square kilometers), but both show the clear need for a better representation of sea ice in fully coupled climate models.

Winter warming (cooling) is amplified as compared to summer warming (cooling) (Bintanja and Van der Linden, 2013). As a result, the seasonal cycle of the temperature is enhanced in colder climates. The amplitude of the seasonal cycle in sea ice area in general does not vary a lot between the climates, with the exception of the 4x CO_2 climate, where the Arctic ocean is almost completely absent of sea ice all year. The seasonal cycle of the sea ice area is, however, potentially dependent on more factors, such as wind patterns (Comiso, 2006), downward longwave radiation fluxes (Francis and Hunter, 2006) and the geometry of the region (Eisenman, 2010).

[1] To validate surface air temperature, data from ERA-Interim (Dee et al., 2011), NCEP / CSFR (Saha et al., 2010) and NASA MERRA-2 (Gelaro et al., 2017) has been used. These are all reanalysis datasets, with values for T_{JJA} of 274.7K, 274.0K and 274.0K respectively. Values for T_{DJF} are 249.1K, 249.4K and 250.9K. For the sea ice area, the observational dataset NSIDC is used. All datasets have been averaged over the period 1990 - 2010.

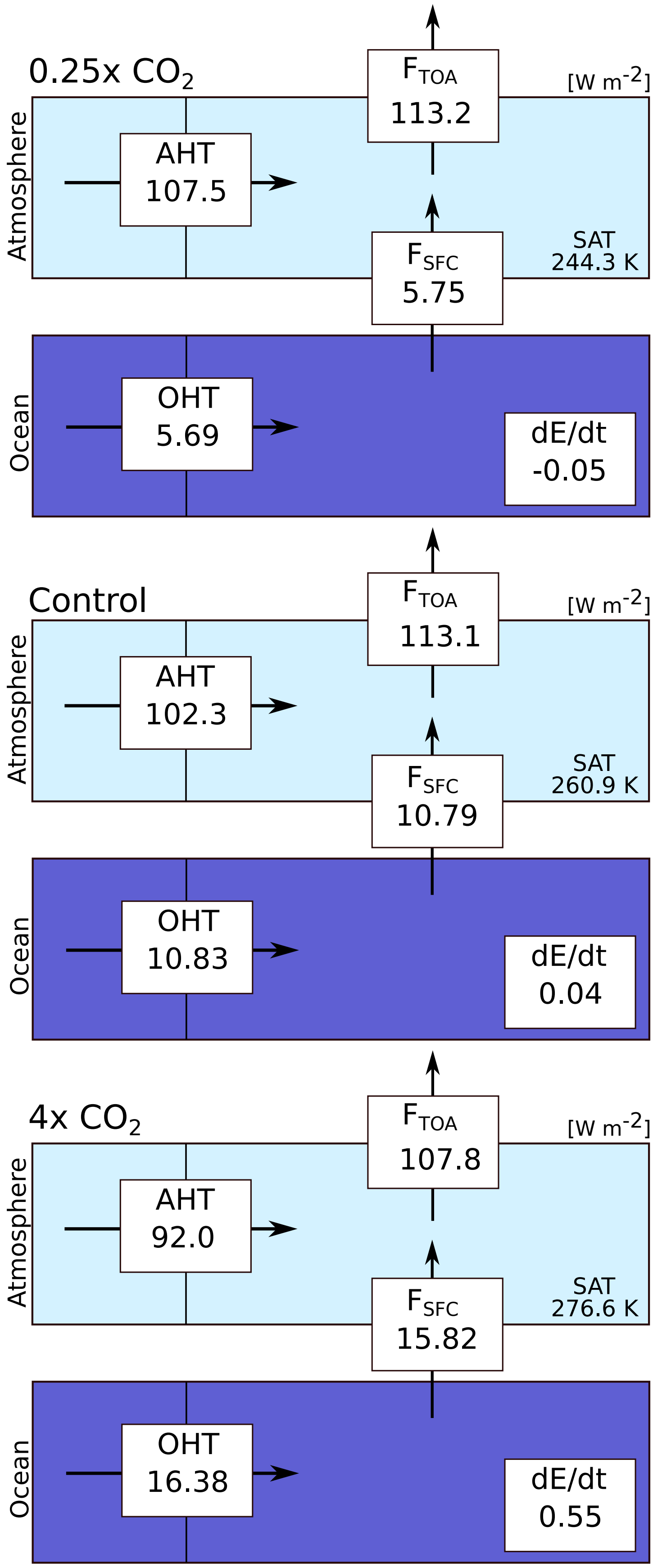

Figure 4 – Schematic of the mean fluxes in and out of the Arctic, as well as the energy heat gain or loss of the ocean. Both are in W m^{-2}. The temperature is indicated in the bottom right of the atmospheric box.

To get an idea of the order of magnitude and direction of the mean fluxes in the Arctic energy budget, box models have been made for the warmest, coldest and control climate. These are shown in Figure 4. The directions of the mean fluxes are the same across all climates. The Arctic region is characterised by a convergence of both the atmospheric and oceanic heat flux, set up by the meridional temperature gradient due to differential heating by the sun. For annual mean fluxes, the convergence of the heat fluxes is primarily compensated by longwave radiation to space (Serreze and Barry, 2011). The annual mean net surface flux is directed upwards. It decreases for colder climates, due to increased sea ice cover inhibiting the exchange of heat between the ocean and the atmosphere. The net flux at the top of the atmosphere (TOA) does not seem to exhibit a trend, although it appears to decrease slightly for warmer climates. This is probably due to the smaller sea ice area, resulting in a lower albedo. A larger fraction of the shortwave radiation is consequently being absorbed at the surface, leading to a smaller net TOA flux.

In the ocean, there is in general a gain of heat for warm climates, very little heat gain or loss for the control climate and heat loss for cold climates, supporting the notion that the ocean is not in equilibrium after the first 100 years. The magnitude of the oceanic transport is clearly smaller than that of the atmospheric heat transport, as is previously observed by Trenberth and Caron (2001). Whereas the mean AHT increases for colder climates, the mean OHT decreases. In colder climates, water temperatures are lower and consequently hold less heat, resulting in a decrease in transport. The larger AHT is due to the increased meridional temperature gradient (Manabe and Wetherald, 1980), arisen because of amplified Arctic warming.

3.1.2 Variability

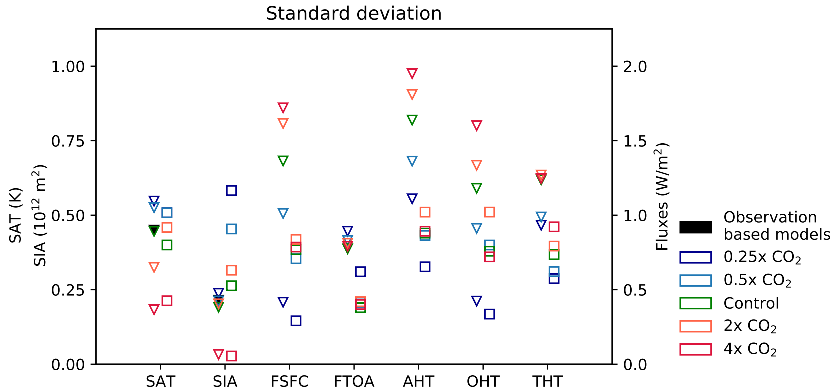

Figure 5 – Standard deviation of the surface air temperature (in K) in the Arctic (70-90°N), the sea ice area (in 10^{12} m^2), the net flux at the surface (F_{sfc}) and at the top of the atmosphere (F_{toa}), both in W m^{-2}. Finally, also the standard deviation of the heat transport through the atmosphere (AHT), through the ocean (OHT) and the total heat transport (THT) are shown, units are also W m^{-2}. Values are annual means, averaged over the Arctic and for interannual (triangles) and decadal (squares) variability. Observation based models have been added (same as described in table 1)[2] to validate surface air temperature and sea ice area variability in the EC-Earth model. The largest common period (1981-2010) is used. These datasets are therefore only suited for validating interannual variability and need to be detrended beforehand.

The standard deviations of annual mean surface air temperature (SAT), sea ice area (SIA) and mean fluxes are shown in Figure 5 for all climate states. Standard deviation in SAT and SIA from observation based models has been added for comparison. Due to the lack of long observational records with good temporal and spatial resolution, only the interannual variability can be assessed in these reanalyses datasets. The interannual variability in temperature of the reanalysis lies exactly on that of the control run. Interannual variability in SAT in the control run of EC-Earth therefore compares well as compared to reanalysis. In a recent study, Rehfeld et al. (2018) examined temperature proxies from the Last Glacial Maximum (about 21 kyr B.P.) to the Holocene (last 11 kyr) and found that, globally, and also in the Arctic itself, variability in SAT decreases towards warmer climates, in accordance with findings here.

For sea ice area, decadal variability is larger than interannual variability. In general, interannual and decadal variability in sea ice area increase towards colder climates, where there is more area and therefore variations in sea ice area can be larger. In addition, in a warming climate, seasonality in ice volume is enhanced, but interannual variability is reduced, until ice-free summers occur (Massonnet et al., 2018). There is, however, an increased variability in the 2x CO_2 run as compared to the control climate on both interannual and decadal timescales, attributed to the the fact that the sea ice on average is thinner, leading to larger variations in sea ice area (van der Linden et al., 2017). The standard deviation in the 4x CO_2 is small, since there is little to no sea ice. Despite the discrepancy in the average sea ice area observed earlier, interannual variability is captured well in the control run of EC-Earth as compared to the observation based datasets.

For surface fluxes, interannual variability is larger than decadal variability. The variability

[2] The values found for the standard deviation of the surface air temperature interannual variations in the reanalyses datasets are 0.47, 0.41 and 0.46K for ERA-Interim, NASA MERRA-2 and NCEP /CSFR, respectively.

in surface fluxes increases towards warmer climates, especially for interannual fluctuations. Variability in net TOA flux does not show a clear dependence on the state of the climate. The larger decadal variability in net TOA flux in the 0.25x CO_2 might be caused by the larger variability in the thermal radiation at the top of the atmosphere, which might be attributed to the larger variability in surface air temperature. The standard deviation of AHT and OHT increases towards warmer climates, especially for interannual variations. In warmer climates, although the mean atmospheric transport poleward decreases, the atmosphere itself can hold more moisture and therefore variations can be larger. Similarly, water temperatures are higher, allowing larger variability in oceanic heat transport.

Since we are limited to one single model, it is useful to validate the representation of the atmospheric dynamics in the EC-Earth model. In order to do this, the AO index has been calculated as the principal component of the first EOF of the mean sea level pressure from 20-90 °N for the control run of the EC-Earth model and for the detrended reanalysis datasets for the period 1981-2010. A regression of the mean sea level pressure on the AO index reveals differences in spatial patterns (Figure 6a-c). Both datasets show a clear anomaly over the central Arctic, with opposite pressure anomalies at lower latitudes on the Atlantic and Pacific side. The anomalies on the Atlantic side and over Siberia are underestimated. Overall, the fingerprint of the AO on the mean sea level pressure is more confined to higher latitudes in EC-Earth as compared to reanalyses datasets. As for the effect of the AO on the temperature, we infer that there is an underestimation of the temperature anomaly over North America and Greenland and a more Northerly extended anomaly over Siberia (Figure 6d-f).

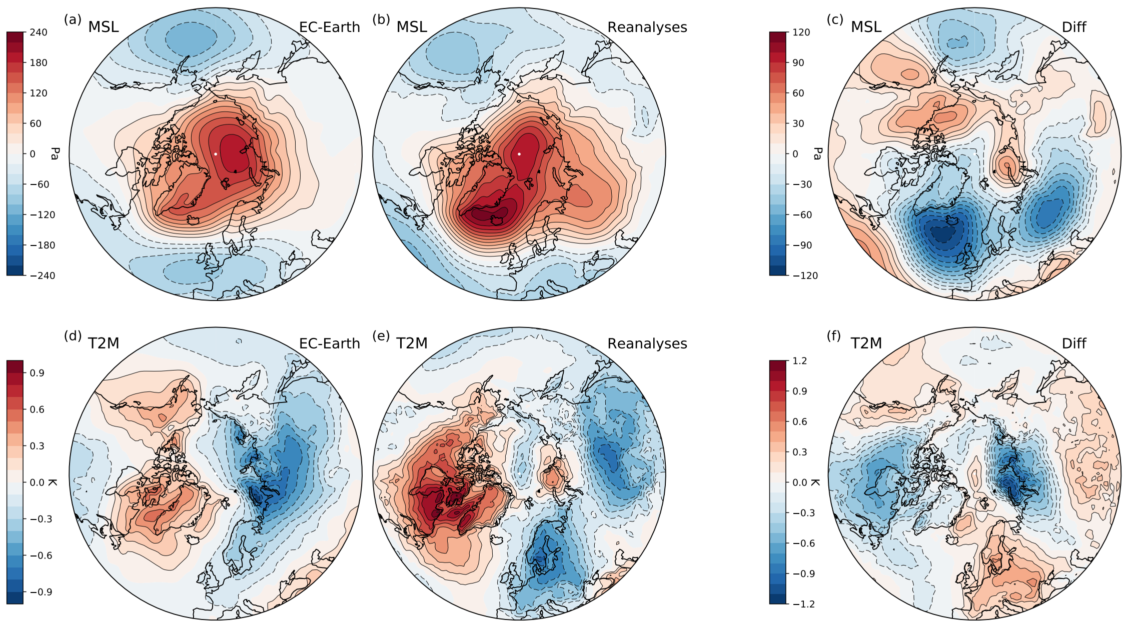

Figure 6 – Regression of the mean sea level pressure (a-c) and the surface air temperature (d-f) on the normalised AO index (the principal component of the first EOF of the mean sea level pressure over 20-90N) in the control run of EC-Earth (a,d), detrended reanalyses data over the period 1981-2010 (b,e) and the difference between the two (c,f).

3.2 Spatial patterns in temperature variability related to poleward heat transport

In the previous sections, we learned that the mean and standard deviation of the Arctic temperature is dependent on the state of the climate. The next step is to look at the processes driving this variability. One of the mechanisms responsible is the meridional heat transport, either through the atmosphere or the oceans. Here, we assess the impact of anomalies in atmospheric and oceanic heat transport on Arctic temperature variability and its dependence on the timescale by looking at regression maps and assessing interannual and decadal variability separately. Most striking patterns are found for regressions on AHT. However, patterns of AHT and OHT are similar, but of opposite sign. For this reason, only plots of the regression on AHT are shown.

Due to its smaller inertia, the atmosphere is expected to control Arctic temperature variations on interannual timescales. Therefore, for interannual variability, positive values are expected when regressing Arctic temperature on AHT through 70 °N. Regression maps of the temperature on the atmospheric heat transport through 70N for interannual variations confirm this (Figure 7). Across all climates, positive values are found over the Arctic ocean, accompanied by small negative values over the Siberian region, thereby bearing resemblance to the imprint of the AO index on the temperature (Figure 6d,e). However, no significant relation has been found between the AO and T2M or AHT on interannual timescales ($r < 0.23$) for the three coldest climates. AO and AHT do exhibit a significant relation for both the 2x CO_2 (r=-0.25) and 4x CO_2 (r=-0.45) climate. In Figure 7, most pronounced positive regressions are found in the 0.25x CO_2 run. Overall, averaged over the Arctic, a positive anomaly in AHT leads to a positive anomaly in SAT for interannual variations.

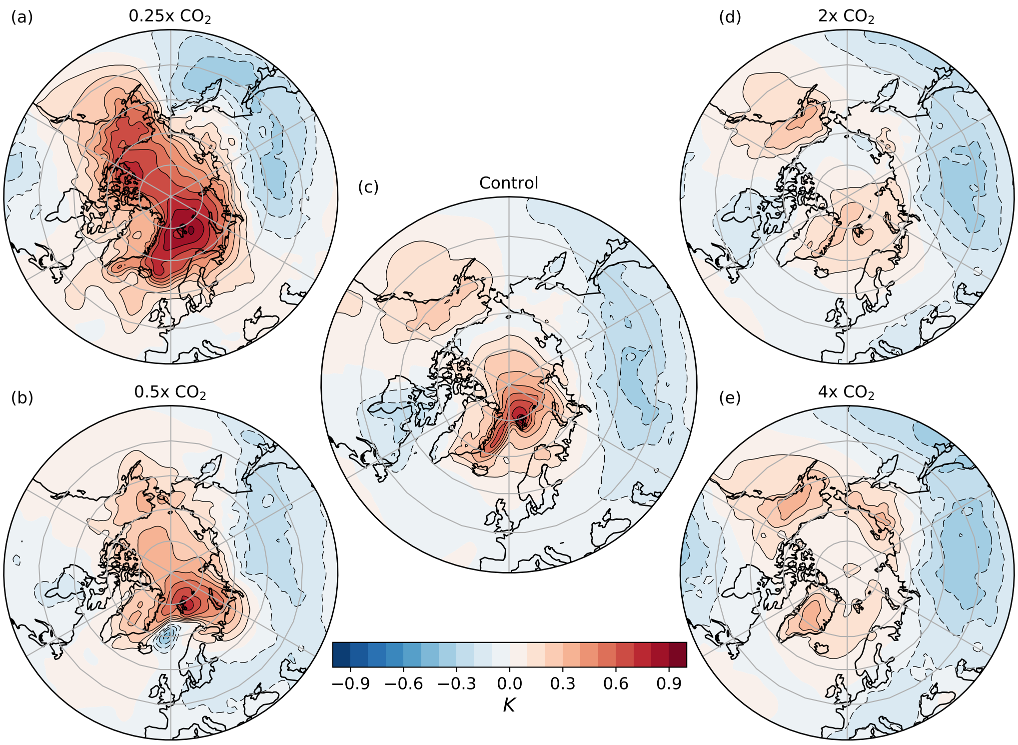

Figure 7 – Regression maps of the temperature on the atmospheric heat transport through 70 °N for interannual variations. Values have been scaled by the standard deviation of AHT.

On decadal timescales, poleward ocean heat transport governs Arctic temperature variability (e.g. Goosse and Holland, 2005; Zhang, 2015; van der Linden et al., 2016). A regression of SAT on OHT results primarily in positive values, concentrated around the sea ice edge (not shown). In these regions, fluctuations in surface fluxes passing on anomalies in OHT are largest and consequently impact surface air temperature variability the most. Regressing AHT through 70° N with temperatures in the Arctic region, on the other hand, show hardly any positive values (Figure 8). In fact, many regions exhibit negative values that arise due to a compensation mechanism known as Bjerknes compensation (Bjerknes, 1964). A positive Arctic temperature anomaly associated with OHT entails a reduction in heat difference between the equator and the poles, resulting in a reduced poleward heat transport through the atmosphere, explaining the negative regression for positive temperature anomalies. However, for the 0.25x CO_2 run, large positive values for the regression of SAT on AHT are found (Figure 8a). Here, the region from 70-90°N is completely covered by sea ice. Therefore, there is little interaction between the atmosphere and the ocean and AHT remains positively correlated with the surface air temperature. In an attempt to find the underlying mechanisms responsible for these positive values, the sensitivity to our choice in area is tested. When the regression is made on AHT through 60°N, the area (now 60-90°N) is in none of the climates fully covered by sea ice and negative values are found across all five climates (not shown). A regression of the temperature on the atmospheric heat transport through 80°N (also not shown), on the other hand, results in positive values for both the 0.25x CO_2 and the 0.5x CO_2 run, since the area from 80 to 90 °N is now completely covered by sea ice in two climates. This shows that the choice of the region in relation to the coverage by sea ice should be taken into account while interpreting these results.

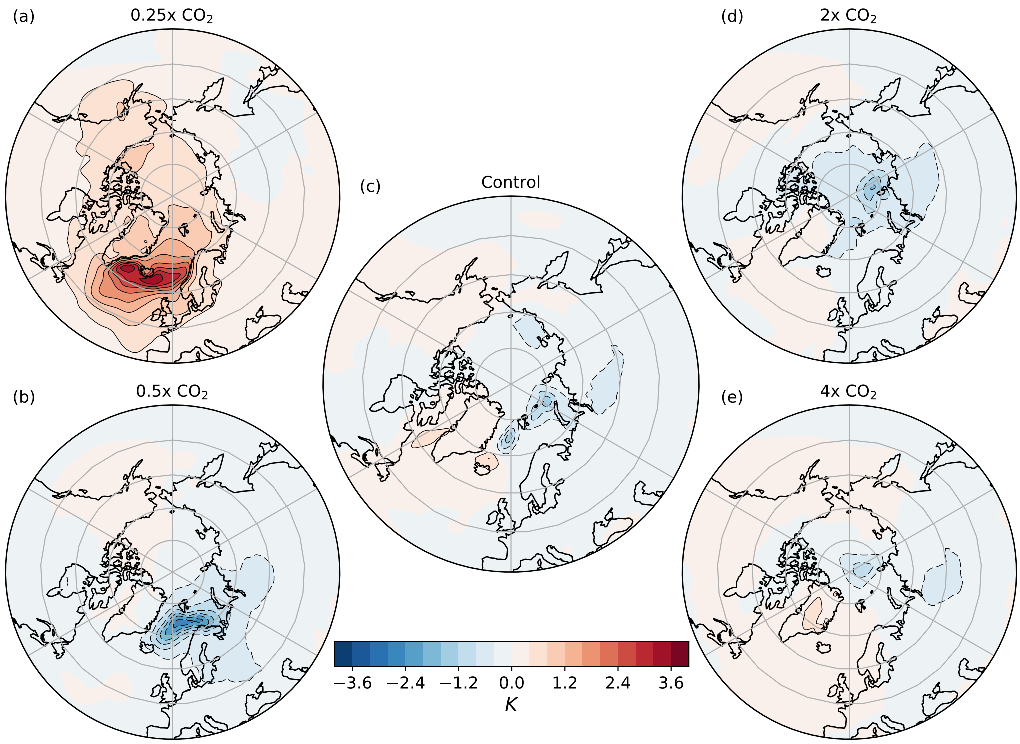

Figure 8 – Regression maps of the temperature on the atmospheric heat transport through 70N for decadal variations. Values have been scaled by the standard deviation of AHT. Note: the scale is four times as large as for interannual variations.

3.3 Timescale dependency

All processes induce variations on their own typical timescale. This is illustrated in Figure 9, which shows correlations between SAT, AHT and OHT as a function of the periodicity. Specific frequency bins are used, filtered by a fifth order Butterworth band-pass filter. In order to get a good resolution for interannual variations, the width of the bins increases logarithmically, ranging from $10^{-2.15}$ - $10^{-1.65}$ yr^{-1} to $10^{-0.55}$ - $10^{-0.05}$ yr^{-1} (corresponding to bins with a period of 45-140 years and 1.1-3.5 years), thereby keeping a constant difference of 0.5 in the exponential. A running correlation is then performed. The frequency assigned to a certain band is that of the average of the minimum and maximum frequency of that band.

Intuitively, on interannual timescales (<10 years), correlations between SAT and AHT would be positive, whereas on decadal timescales (>10 years), correlations between SAT and OHT are expected to be positive, as explained earlier. For positive correlations, a positive (negative) anomaly in SAT is associated with a larger (smaller) poleward AHT. For the 0.5x CO_2, the control and the 2x CO_2 run, this holds. For the other two runs, the Arctic stands out by either being fully covered by sea ice (0.25x CO_2) or by being completely devoid of sea ice, thereby impacting large-scale dynamics. In a fully covered Arctic, the presence of sea ice inhibits exchange of heat and moisture between the ocean and the atmosphere. This puts a limit on the amount of heat that can be passed on from the Arctic ocean to the atmosphere and vice versa. Variability in surface air temperature consequently remains associated to variations in atmospheric transport on all timescales (Figure 9b). In an Arctic completely absent of sea ice, ocean heat transport is not significantly correlated to the surface air temperature on all timescales. Large-scale atmospheric and oceanic circulation changes might be at play here (Mayewski et al., 2004). Density profiles might provide more insight in what is happening in this warm climate. In such a warm climate, sea surface temperatures are no longer restricted to the melting point temperature and much higher values can be reached, thus decreasing the density at the surface (supplementary Figures 1,2). Moreover, while transitioning to this climate state, melting sea ice freshens the upper ocean, resulting in even lower densities. With such low surface densities, vertical mixing is likely to be limited, impacting surface fluxes and hence surface air temperatures. However, the 4x CO_2 run in Figure 9a does not differ from that in the climates containing 0.5x, 1x and 2x CO_2, so it appears the relation between atmospheric transport and temperature variability has not changed drastically as compared to the other climates. Further research needs to be done to test the robustness of this hypothesis.

The previously described Bjerknes compensation (Bjerknes, 1964) explains the negative correlations between the surface air temperature and the atmospheric heat transport. This compensation mechanism is evident from Figure 9c, which shows large negative correlations between AHT and OHT, especially on decadal timescales. For the two most extreme climates, correlations are smaller in magnitude (although mostly still significant). According to Jungclaus and Koenigk (2010), the presence or absence of Bjerknes compensation is largely determined by large-scale atmospheric circulations in the Pacific sector of the Arctic. Spatially, the maximum Bjerknes compensation rate is found to be in regions containing seasonal sea ice (Van der Swaluw et al., 2007). This potentially hints at an important role of sea ice variability for Bjerknes compensation.

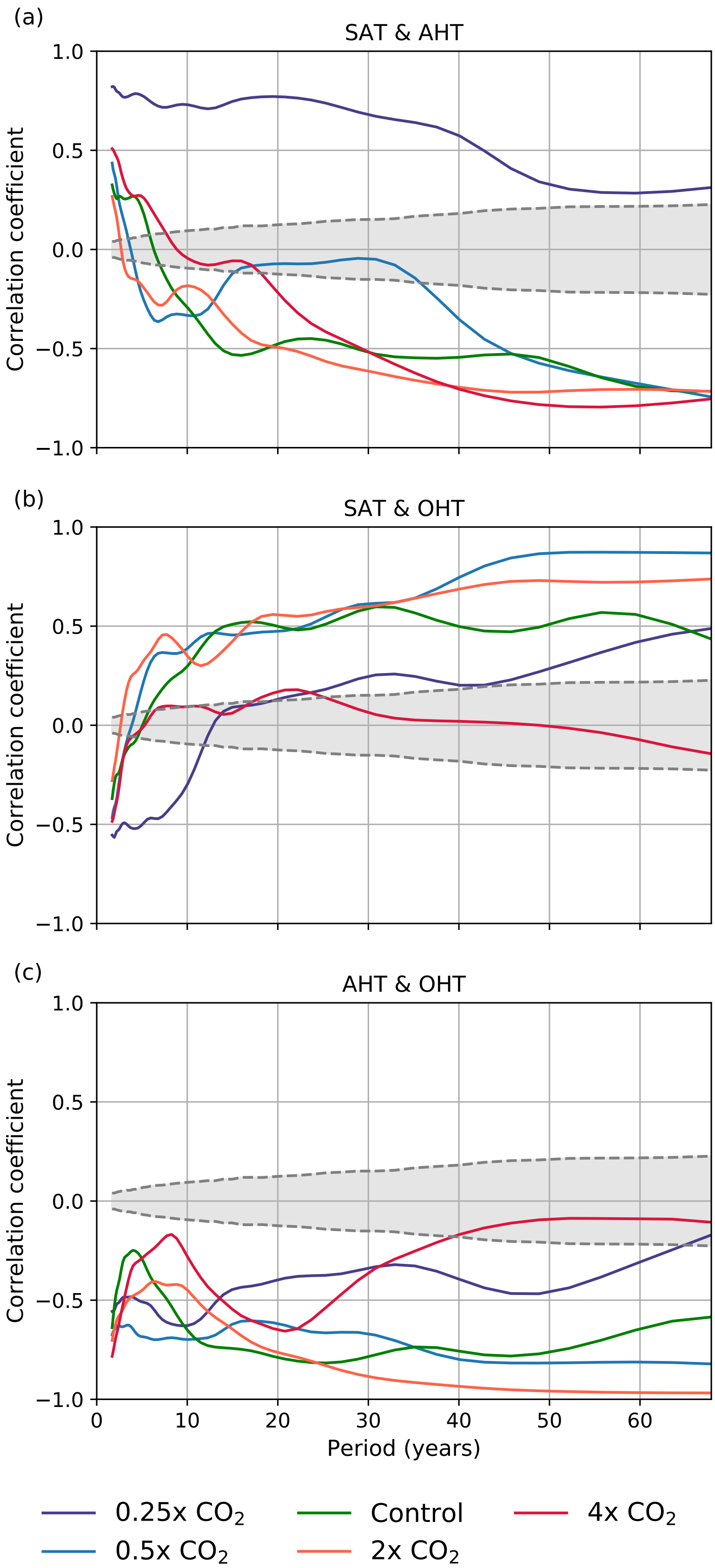

Figure 9 – Correlation for variations on specific frequency bins as a function of periodicity. The period on the x-axis denotes the central period of the window used. The shaded area indicates the region where correlations are insignificant as determined by bootstrapping the data 1000 times before applying a frequency filter.

3.4 The role of sea ice

Since sea ice cover governs the interaction between atmosphere and ocean with regard to variability on various time scales, we will test the effect of sea ice extent on the various correlations. As the difference between the 0.25x CO_2 and the other runs is largest on decadal timescales, Figure 10 shows the correlation coefficient between AHT through a specific latitude and SAT in the Arctic for decadal variability. The circles and squares denote the latitude of the sea ice edge on the Atlantic side (60°W-30°E), where the sea ice edge is defined by the 15% and 90% isopleth, respectively. Because smoothing raises the correlation, a bootstrap significance test with 1000 samples has been done. Correlations are found to be significant above 0.35.

The three coldest climates exhibit a sudden increase in correlation towards the Arctic. The range of latitudes that span this transition varies from 60-70°N in the 0.25x CO_2 climate to 80-85°N in the control climate. We infer that positive correlations are found between AHT and SAT from this latitude onward, also on decadal timescales. At these latitudes, the sea ice present is perennial and inhibits exchange from the ocean to the atmosphere all year round. This is in agreement with results discussed in section 3.2. The absence of a sudden increase in the two warm climates is due to the absence of perennial ice. Negative correlations at lower latitudes are likely a result of the previously described Bjerknes compensation.

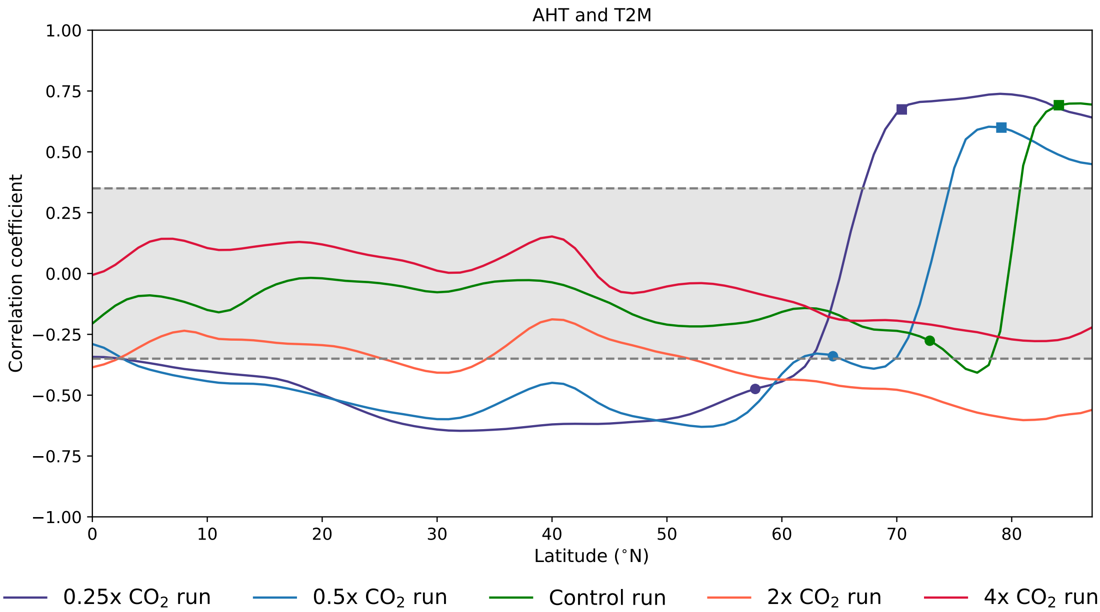

Figure 10 – Correlation between AHT through a latitude (indicated on the x-axis) and the average temperature in the Arctic (70-90 °N) for variations on decadal timescales. The dots and the squares indicate the average latitude of the sea ice edge on the Atlantic side (60°W-30°E), where the edge is defined as the 15 % and 90 % isopleth, respectively. Insignificant correlations are shaded.

3.5 Leads and lags

Even though correlations are insightful to identify possible climate links behind Arctic variability, studying leads/lags will provide better insight into the governing physical mechanisms. Figure 11 shows the correlation between two variables for different leads and lags. In order to calculate the lag in months, a 12 month running mean has been applied to the data. For positive lags, the first variable mentioned is leading. The significant maxima and minima are denoted by the circles.

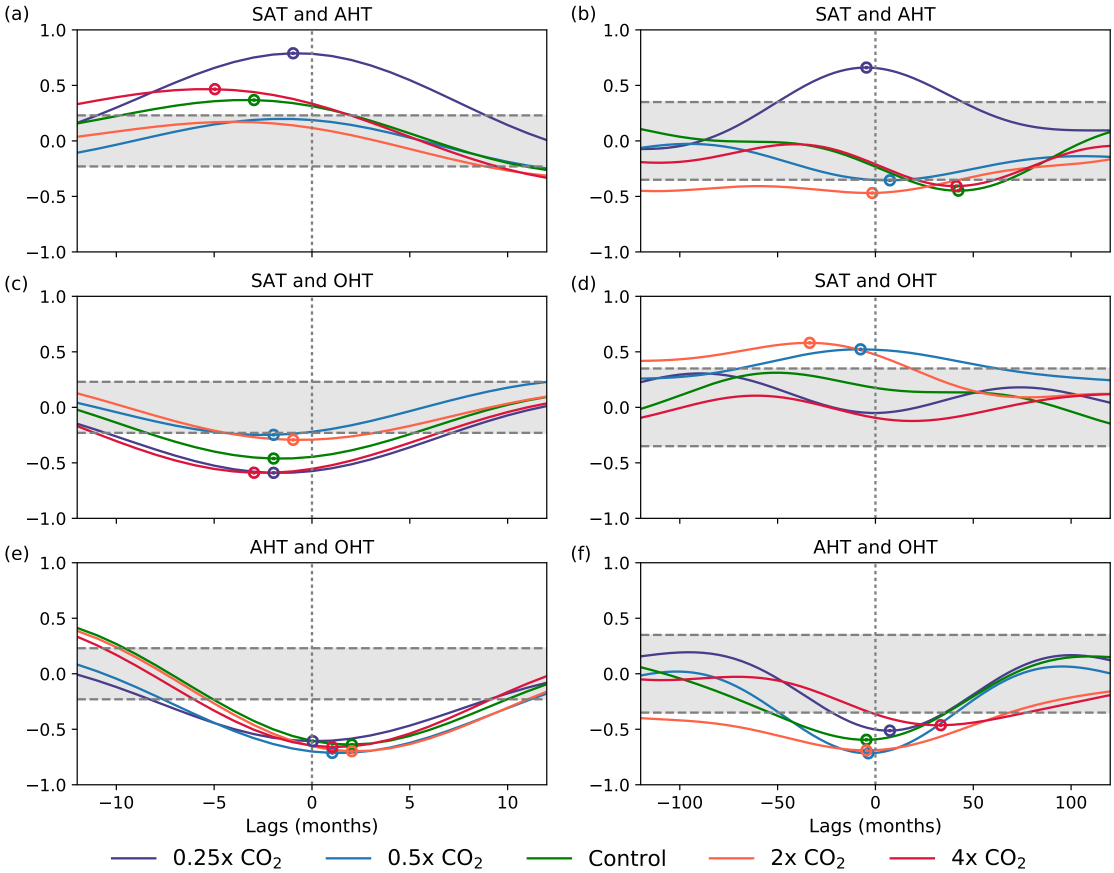

Figure 11 – Correlation between SAT, AHT and OHT for different leads / lags when low frequencies (left) and high frequencies (right) are selected. At positive lags the first variable mentioned is leading. The dashed horizontal lines mark the limits of correlations that could arise due to the filtering of frequencies. The open circles represent the significant maximum correlations. Between -0.35 and 0.35, correlations for decadal variability are insignificant, indicated by the shaded area. For interannual variations, this is between -0.23 and 0.23. Note the difference in scale on the x-axes.

Leads and lags for interannual variability (Figure 11, left-hand side panels) are consistent across all climates. Clearly, the atmosphere leads temperature variability (Figure 11a). Significant correlations are found for the 0.25x CO_2, the control and the 4x CO_2 run, with a maximum value for an atmosphere leading by 1, 3 and 5 months, respectively. Across all climates, OHT leads SAT, with negative correlations up to -0.59 in the 0.25x CO_2 and 4x CO_2 run (Figure 11b). This suggests that both the atmosphere and the ocean are leading with respect to fluctuations in temperature. Taking a look at Figure 11c reveals that it is the atmosphere who leads variations in ocean heat transport. To conclude, variations in atmospheric heat transport drive both variations in SAT and OHT on interannual timescales, where the response time of the ocean is smaller than that of the temperature.

Decadal variability exhibits a somewhat different picture (Figure 11, right-hand side panels). Now, instead, surface air temperature leads atmospheric heat transport (aside from the 2x CO_2 and 0.25x CO_2 climates) (Figure 11b). The atmosphere responds by modifying its pressure patterns (Jungclaus and Koenigk, 2010), resulting in anomalous heat flow. The largest correlations are found for lags ranging from about 7 months in the 0.5x CO_2 run to 3.5 years in the control and 4x CO_2 run. The positive correlations found between AHT and SAT in the coldest climate are explained earlier (see section 3.2). Also, in this run, the atmosphere still leads the temperature variations. Correlations between ocean heat transport and surface air temperature are largest when the ocean heat transport is leading and only significant for the 2x CO_2 and 0.5x CO_2, emphasizing the modified role of the oceans in the two extreme climates. These two extreme climates also exhibit a leading atmosphere with respect to oceanic heat transport (Figure 11f). For the other climates, OHT leads AHT, although there are differences in response times. In the 2x CO_2 run, for example, the atmosphere seems to respond faster than the temperature.

4 Discussion and conclusion

In this study, the dependence of Arctic variability on the timescale and the state of the climate is investigated using five simulations with 0.25x, 0.5x, 1x, 2x and 4x the present-day CO_2 concentration. This paper focuses on the link between Arctic temperature variability and heat transport towards the Arctic through the atmosphere and the oceans and its dependence on the climate state. Variability on timescales ranging from interannual to (multi-)decadal are considered.

Assessing interannual to decadal variability of long observational records is difficult, since the temporal resolution of proxies is too coarse. We therefore rely on models and the model physics and parameterisations inherent in these models, especially when using only one model.

In determining the origin of Arctic temperature variability, an attempt has been made to link temperature variability to anomalies in heat transport. First, the mean state is investigated. On average, atmospheric heat transport decreases towards warmer climates, whereas oceanic heat transport increases. In a warmer climate, the meridional temperature gradient between the equator and the poles is decreased because of the well-known Arctic amplification mechanism (Holland and Bitz, 2003), reducing the annual mean atmospheric heat transport. In the ocean, the higher water temperatures enable the transport of more heat. Coherently, variability in poleward ocean heat transport increases in warmer climates. Variability in atmospheric heat transport increases towards warmer climate states, most likely due to the increased moisture holding capacity of a warmer atmosphere, in contrast to the average atmospheric heat transport. These variability trends are most clear on interannual timescales. On decadal timescales, the results are more ambiguous, hampering the ability to draw any conclusions.

Evidently, Arctic temperature variability highly depends on the state of the climate, with interannual variability in surface air temperature increasing towards colder climates. Decadal variability in general follows the same pattern, with the exception of an increase in variability in the 2x CO_2 run, caused to a large extent by the increased decadal variability in the surface fluxes. For sea ice variability, many factors are involved (Comiso, 2006; Francis and Hunter, 2006; Eisenman, 2010). Its central role is only more confirmed here, as is evident by the strong coupling between temperature and sea ice area, mostly through its impact on the surface fluxes (Selivanova et al., 2016). As we have seen, this coupling also determines to which extent oceanic and atmospheric heat transport modulate the variability in Arctic temperature on decadal timescales. Sea ice acts as a lit, inhibiting exchange between the ocean and the atmosphere. In a climate in which the Arctic is fully covered by sea ice, this lit prevents the ocean to pass along its variability to the atmosphere. As a result, it leaves the atmosphere to be driving variability also on decadal timescales. In an Arctic devoid of sea ice, ocean heat transport does not show a correlation to Arctic surface air temperature variability on any timescale. In such a warm climate, density profiles become more stable and mixing is likely limited (supplementary Figures 1,2), with the result that poleward heat transport variations are no longer passed on as well. This hypothesis, however, needs to be tested more thoroughly before drawing any conclusions.

To put this in the perspective of previous research, this paper shows the clear difference and need to distinguish between interannual and decadal variability of temperature and sea ice area. Variability on both interannual (e.g. Zhang and Li, 2017; Caian et al., 2018) and decadal (e.g. Day et al., 2012; van der Linden et al., 2017) timescales have been investigated seperately, but this is the first time that its timescale dependence is quantified. We acknowledge that these results are solely based on the EC-Earth model. Nevertheless it helps gain better insight in how variability may change depending on its timescale and the state of the climate.

References

Marius Årthun and Tor Eldevik. On anomalous ocean heat transport toward the arctic and associated climate predictability. *Journal of Climate*, 29(2):689–704, 2016.

Gianpaolo Balsamo, Anton Beljaars, Klaus Scipal, Pedro Viterbo, Bart van den Hurk, Martin Hirschi, and Alan K Betts. A revised hydrology for the ecmwf model: Verification from field site to terrestrial water storage and impact in the integrated forecast system. *Journal of hydrometeorology*, 10(3):623–643, 2009.

Richard Bintanja and EC Van der Linden. The changing seasonal climate in the arctic. *Scientific reports*, 3:1556, 2013. doi: 10.1038/srep01556.

Richard Bintanja, Roderik SW van de Wal, and Johannes Oerlemans. Modelled atmospheric temperatures and global sea levels over the past million years. *Nature*, 437 (7055):125, 2005.

Jf Bjerknes. Atlantic air-sea interaction. In *Advances in geophysics*, volume 10, pages 1–82. Elsevier, 1964.

Mihaela Caian, Torben Koenigk, Ralf Döscher, and Abhay Devasthale. An interannual link between arctic sea-ice cover and the north atlantic oscillation. *Climate Dynamics*, 50(1-2):423–441, 2018.

P Chylek, J Li, MK Dubey, M Wang, and G Lesins. Observed and model simulated 20th century arctic temperature variability: Canadian earth system model canesm2. *Atmospheric Chemistry and Physics Discussions*, 8:22893–22907, 2011.

Josefino C Comiso. Abrupt decline in the arctic winter sea ice cover. *Geophysical Research Letters*, 33(18), 2006.

Josefino C Comiso and Dorothy K Hall. Climate trends in the arctic as observed from space. *Wiley Interdisciplinary Reviews: Climate Change*, 5(3):389–409, 2014.

JJ Day, JC Hargreaves, JD Annan, and A Abe-Ouchi. Sources of multi-decadal variability in arctic sea ice extent. *Environmental Research Letters*, 7(3):034011, 2012.

Dick P Dee, SM Uppala, AJ Simmons, Paul Berrisford, P Poli, S Kobayashi, U Andrae, MA Balmaseda, G Balsamo, d P Bauer, et al. The era-interim reanalysis: Configuration and performance of the data assimilation system. *Quarterly Journal of the royal meteorological society*, 137(656):553–597, 2011.

Henk Dijkstra. *Dynamical oceanography*. Springer Verlag, Berlin, 2008. ISBN 9783540763758.

Ian Eisenman. Geographic muting of changes in the arctic sea ice cover. *Geophysical Research Letters*, 37(16), 2010.

Thierry Fichefet and MA Maqueda. Sensitivity of a global sea ice model to the treatment of ice thermodynamics and dynamics. *Journal of Geophysical Research: Oceans*, 102 (C6):12609–12646, 1997.

Christopher B Field, Vicente R Barros, K Mach, and M Mastrandrea. *Climate change 2014: impacts, adaptation, and vulnerability*, volume 1. Cambridge University Press Cambridge and New York, 2014.

Jennifer A Francis and Elias Hunter. New insight into the disappearing arctic sea ice. *Eos, Transactions American Geophysical Union*, 87(46):509–511, 2006.

Claude Frankignoul, Nathalie Sennéchael, and Pierre Cauchy. Observed atmospheric response to cold season sea ice variability in the arctic. *Journal of Climate*, 27(3):1243–1254, 2014.

Andrey Ganopolski, Stefan Rahmstorf, Vladimir Petoukhov, and Martin Claussen. Simulation of modern and glacial climates with a coupled global model of intermediate complexity. *Nature*, 391(6665):351, 1998.

Ronald Gelaro, Will McCarty, Max J Suárez, Ricardo Todling, Andrea Molod, Lawrence Takacs, Cynthia A Randles, Anton Darmenov, Michael G Bosilovich, Rolf Reichle, et al. The modern-era retrospective analysis for research and applications, version 2 (merra-2). *Journal of Climate*, 30(14):5419–5454, 2017.

H. Goosse and T. Fichefet. Importance of ice-ocean interactions for the global ocean circulation: A model study. *Journal of Geophysical Research: Oceans*, 104(C10):23337–23355, 1999. ISSN 2156-2202. doi: 10.1029/1999JC900215.

Hugues Goosse and Marika M Holland. Mechanisms of decadal arctic climate variability in the community climate system model, version 2 (ccsm2). *Journal of climate*, 18(17): 3552–3570, 2005.

James Hansen, Reto Ruedy, Mki Sato, and Ken Lo. Global surface temperature change. *Reviews of Geophysics*, 48(4), 2010.

W Hazeleger, X Wang, C Severijns, S Ştefănescu, R Bintanja, A Sterl, Klaus Wyser, T Semmler, S Yang, B Van den Hurk, et al. Ec-earth v2. 2: description and validation of a new seamless earth system prediction model. *Climate dynamics*, 39(11):2611–2629, 2012.

Marika M Holland. The north atlantic oscillation–arctic oscillation in the ccsm2 and its influence on arctic climate variability. *Journal of Climate*, 16(16):2767–2781, 2003.

Marika M Holland and Cecilia M Bitz. Polar amplification of climate change in coupled models. *Climate Dynamics*, 21(3-4):221–232, 2003.

James W Hurrell, Yochanan Kushnir, Geir Ottersen, and Martin Visbeck. An overview of the north atlantic oscillation. *The North Atlantic Oscillation: climatic significance and environmental impact*, pages 1–35, 2003.

Johann H Jungclaus and Torben Koenigk. Low-frequency variability of the arctic climate: the role of oceanic and atmospheric heat transport variations. *Climate dynamics*, 34 (2-3):265–279, 2010.

Christophe Kinnard, Christian M Zdanowicz, David A Fisher, Elisabeth Isaksson, Anne de Vernal, and Lonnie G Thompson. Reconstructed changes in arctic sea ice over the past 1,450 years. *Nature*, 479(7374):509, 2011.

G. Madec. *NEMO ocean engine*. Note du Pôle de modélisation, Institut Pierre-Simon Laplace (IPSL), France, No 27, ISSN No 1288-1619, 2008.

Syukuro Manabe and Richard T Wetherald. On the distribution of climate change resulting from an increase in co2 content of the atmosphere. *Journal of the Atmospheric Sciences*, 37(1):99–118, 1980.

Nathan J Mantua and Steven R Hare. The pacific decadal oscillation. *Journal of oceanography*, 58(1):35–44, 2002.

François Massonnet, Martin Vancoppenolle, Hugues Goosse, David Docquier, Thierry Fichefet, and Edward Blanchard-Wrigglesworth. Arctic sea-ice change tied to its mean state through thermodynamic processes. *Nature Climate Change*, page 1, 2018.

Paul A Mayewski, Eelco E Rohling, J Curt Stager, Wibjörn Karlén, Kirk A Maasch, L David Meeker, Eric A Meyerson, Francoise Gasse, Shirley van Kreveld, Karin Holmgren, et al. Holocene climate variability. *Quaternary research*, 62(3):243–255, 2004.

Noboru Nakamura and Abraham H Oort. Atmospheric heat budgets of the polar regions. *Journal of Geophysical Research: Atmospheres*, 93(D8):9510–9524, 1988. doi: 10.1029/jd093id08p09510.

Joseph Ortiz, Tom Guilderson, Michael Sarnthein, et al. Coherent high-and low-latitude climate variability during the holocene warm period. *Science*, 288(5474):2198–2202, 2000.

Kira Rehfeld, Thomas Münch, Sze Ling Ho, and Thomas Laepple. Global patterns of declining temperature variability from the last glacial maximum to the holocene. *Nature*, 554(7692):356, 2018.

D Rind, R Healy, C Parkinson, and D Martinson. The role of sea ice in 2× co2 climate model sensitivity: Part ii: Hemispheric dependencies. *Geophysical Research Letters*, 24 (12):1491–1494, 1997.

Suranjana Saha, Shrinivas Moorthi, Hua-Lu Pan, Xingren Wu, Jiande Wang, Sudhir Nadiga, Patrick Tripp, Robert Kistler, John Woollen, David Behringer, et al. The ncep climate forecast system reanalysis. *Bulletin of the American Meteorological Society*, 91 (8):1015–1058, 2010.

James A Screen and Ian Simmonds. The central role of diminishing sea ice in recent arctic temperature amplification. *Nature*, 464(7293):1334, 2010.

JV Selivanova, ND Tilinina, SK Gulev, and SA Dobrolubov. Impact of ice cover in the arctic on ocean–atmosphere turbulent heat fluxes. *Oceanology*, 56(1):14–18, 2016.

Mark C Serreze and Roger G Barry. Processes and impacts of arctic amplification: A research synthesis. *Global and Planetary Change*, 77(1-2):85–96, 2011.

Mark C Serreze, Andrew P Barrett, Andrew G Slater, Michael Steele, Jinlun Zhang, and Kevin E Trenberth. The large-scale energy budget of the arctic. *Journal of Geophysical Research: Atmospheres*, 112(D11), 2007.

Karl E Taylor, Ronald J Stouffer, and Gerald A Meehl. An overview of cmip5 and the experiment design. *Bulletin of the American Meteorological Society*, 93(4):485–498, 2012.

Kevin E Trenberth and Julie M Caron. Estimates of meridional atmosphere and ocean heat transports. *Journal of Climate*, 14(16):3433–3443, 2001.

S Valcke, A Caubel, D Declat, and L Terray. Oasis3 ocean atmosphere sea ice soil user's guide. *Prisim project report*, 2, 2003.

Eveline C van der Linden, Richard Bintanja, Wilco Hazeleger, and Rune G Graversen. Low-frequency variability of surface air temperature over the barents sea: causes and mechanisms. *Climate dynamics*, 47(3-4):1247–1262, 2016.

Eveline C. van der Linden, Richard Bintanja, and Wilco Hazeleger. Arctic decadal variability in a warming world. *Journal of Geophysical Research: Atmospheres*, 122(11): 5677–5696, jun 2017. doi: 10.1002/2016jd026058.

E Van der Swaluw, SS Drijfhout, and W Hazeleger. Bjerknes compensation at high northern latitudes: the ocean forcing the atmosphere. *Journal of climate*, 20(24):6023–6032, 2007.

Lei Zhang and Tim Li. Physical processes responsible for the interannual variability of sea ice concentration in arctic in boreal autumn since 1979. *Journal of Meteorological Research*, 31(3):468–475, 2017.

Rong Zhang. Mechanisms for low-frequency variability of summer arctic sea ice extent. *Proceedings of the National Academy of Sciences*, 112(15):4570–4575, 2015.

5 Supplementary Figures

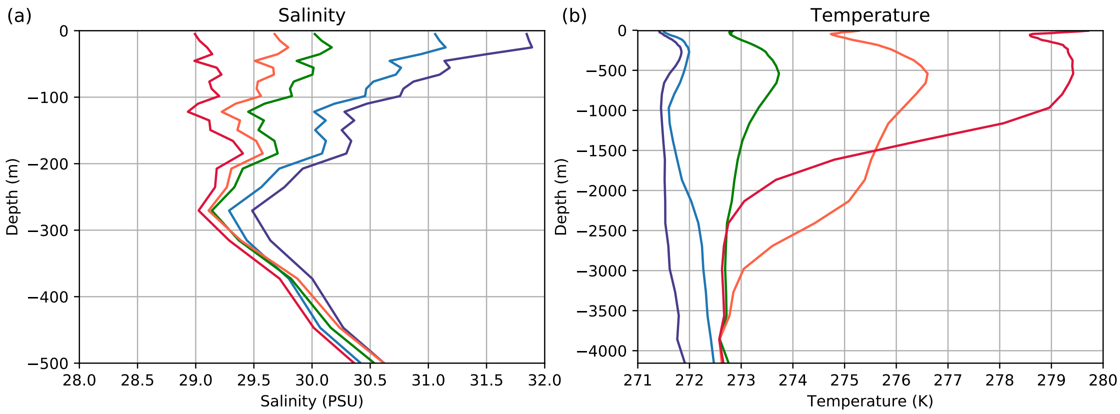

Figure 12 – Average Arctic ocean temperature (a) and salinity (b) as a function of depth. Temperatures in the 4x CO_2 climate are able to reach much higher values, because of the absence of sea ice (more energy can be used to heat the water). Salinity difference are most pronounced in the first few hundred meters (note the y-axes). On average, Salinity becomes smaller towards warmer climates.

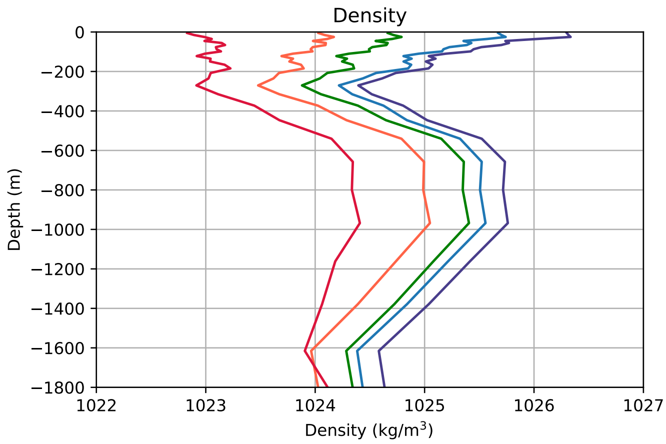

Figure 13 – Average Arctic ocean density as a function of depth. Density at the surface becomes lower towards warmer climates, resulting in a more stable profile.